

Real photoabsorption and the proton structure function at low x

P. Moseley and G. Shaw

*Department of Physics and Astronomy, Schuster Laboratory, University of Manchester,
Manchester M13 9PL, United Kingdom*

(Received 12 June 1995)

We investigate real photoabsorption and proton structure function data from the laboratory frame viewpoint, in which the x dependence reflects the space-time structure of the process. Both the real and virtual photon data are well described by a simple model in which the striking enhancement observed at DESY HERA at very low x and high Q^2 is associated with contributions from heavy long-lived fluctuations of the incoming photon. As Q^2 becomes smaller, the effect is predicted to decrease rapidly and shift towards $x = 0$.

PACS number(s): 13.60.Hb, 12.40.Vv, 14.20.Gk

I. INTRODUCTION

In this paper we consider the high energy behavior of the total photoabsorption cross section combination

$$\sigma_{\gamma p}(\nu, Q^2) = \sigma_T(\nu, Q^2) + \sigma_S(\nu, Q^2)$$

and the associated small x behavior of the proton structure function, which is given by

$$F_2(x, Q^2) = \frac{Q^2}{4\pi^2\alpha} \sigma_{\gamma p}(\nu, Q^2)$$

for large $\nu \gg 2Mx$. They are conveniently characterized by the Regge-pole-inspired parametrization

$$\sigma_{\gamma p}(\nu, Q^2) \approx a_P(Q^2)\nu^{\alpha_P-1} + a_R(Q^2)\nu^{\alpha_R-1}$$

which implies

$$F_2(x) \approx \tilde{a}_P x^{1-\alpha_P} + \tilde{a}_R x^{1-\alpha_R} \quad (1)$$

in the scaling region. Interest centers on the observed behavior of the effective Pomeron intercept α_P . For real photons, the data are consistent with the typical hadronic behavior [1] $\alpha_P \approx 1.08$ and the same behavior is consistent [2] with structure function data in the intermediate x -region $0.02 \leq x \leq 0.1$. However experiments at the DESY ep collider HERA [3–5] observe a sharp rise in the structure function at small $x < 0.02$ which can be parametrized using an effective intercept $\alpha_P \approx 1.3$ [6]. Theoretical discussion of this effect usually centers on perturbative QCD, and in particular on the prediction $\alpha_P \approx 1.5$ obtained in the leading $\ln(1/x)$ approximation [7]. However such discussions are normally restricted to large Q^2 , and cannot be easily extended to low Q^2 and real photons. They cannot lead to a parametrization valid for all Q^2 , which is required, for example, in calculating radiative corrections; and they cannot shed light on the transition between the contrasting energy dependences observed for real and highly virtual photons, which is one of the most interesting features of the data.

Here we consider a complementary approach suggested by one of us [8] which adopts the laboratory frame view-

point of hadron dominance models. Such models emphasize the link between real and virtual photons and provide a natural framework for describing the onset of scaling. For example, they give a good description of elastic ρ -meson production for both real and highly virtual photons; they provide an interpolation between real photoabsorption and deep inelastic scattering data on protons in the intermediate x -region $0.02 \leq x \leq 0.1$; and they successfully predict the observed shadowing behavior for real photoabsorption and deep inelastic scattering on nuclei in the same kinematic region.¹ The suggestion [8] was that this approach could be extended into the ‘‘HERA’’ region $x \lesssim 0.01$ if the observed low x rise is associated with the contribution of high mass fluctuations of the photon which become important at high Q^2 . The discussion centered on the value of the coherence length:²

$$l = \frac{2\nu}{m^2 + Q^2} = \frac{1}{Mx} \frac{1}{1 + m^2/Q^2}, \quad (2)$$

which represents the typical distance traveled by a fluctuation of mass m in the laboratory frame. At short coherence lengths, corresponding to large x values $x > 0.1$, these states are essentially bare $\bar{q}q$ pairs and a hadronic component of the photon has not developed. At moderate coherence lengths, corresponding typically to intermediate x values $0.02 < x < 0.1$ for typical masses $m^2 \approx Q^2$, they are assumed to have the single hadron-like behavior expected for constituent $\bar{q}q$ pairs or vector mesons. However at very small x the photon fluctuations can be very long lived, for example, $l \sim 100$ fm for $x \sim 10^{-3}$ and $m \sim Q^2$, and it is plausible to assume that they can develop into the hadronic final states ob-

¹For recent discussions of these points, and many earlier references, see [8, 9] (elastic ρ production), [8, 10] (real and virtual photoabsorption); and [11, 12] (nuclear shadowing).

²For an interesting discussion of the role of the coherence length in another context, see Del Duca, Brodsky, and Hoyer [13].

served in e^+e^- annihilations. For low masses, these can be approximated by a sum of vector mesons; but for high masses complicated multihadron jetlike structures are observed. The proposal [8] was that the aforementioned rise in F_2 at small x is associated with just these multihadron states, but only a brief qualitative discussion was given. Here we investigate whether this idea can quantitatively describe both the photoproduction and structure function data in the framework of a simple model. Further, since the nature of the interaction of such complicated intermediate states with the proton is far from clear, we shall assume two simple but contrasting behaviors to see how this affects the fits to the data, and the predictions in the interesting but experimentally unexplored intermediate Q^2 region.

To do this, we adopt a two-stage approach. The idea is that the new phenomena are associated with multihadron states which can only play a role for masses m and coherence lengths l which are greater than some critical values $m > m_J$ and $l > l_c$. By (2) this implies that they are confined to energies

$$\nu > \nu_c \equiv m_J^2 l_c / 2 \quad (Q^2 = 0), \quad (3)$$

in photoproduction, and to the kinematic region

$$x < x_c(Q^2) \equiv \frac{1}{M l_c} \frac{Q^2}{Q^2 + m_J^2} \quad (4)$$

for structure functions. Taking the reasonable values $m_J^2 = 10 \text{ GeV}^2$ and $l_c = 10 \text{ fm}$ for example gives $\nu_c = 250 \text{ GeV}$ and $x_c(10 \text{ GeV}^2) = 0.01$. We therefore first formulate a hadron dominance model—the simplest we can think of—and adjust its parameters to fit “pre-HERA” data in regions $\nu < \nu_c$ for $Q^2 = 0$ and $x > x_c(Q^2)$ for $Q^2 \neq 0$; and then introduce the suggested high mass, long coherence length effects to extend it into the new kinematic regions explored by HERA.

II. THE FORM OF THE PARAMETRIZATION

In the hadron dominance model,³ the total cross section for photoabsorption is given by an expression of the form

$$\sigma_{\gamma p}(\nu, Q^2) = \int dm^2 \int dm'^2 \frac{\rho(m, m', s)}{(m^2 + Q^2)(m'^2 + Q^2)} \quad (5)$$

corresponding to Fig. 1. The main contributions are expected to come from elastic and near elastic components in which the two mass values m and m' are not very different. Equation (5) is therefore often replaced by a simple diagonal approximation

$$\sigma_{\gamma p}(\nu, Q^2) = \int_{m_0^2}^{\infty} dm^2 \frac{\rho(\nu, m^2)}{(m^2 + Q^2)^2}, \quad (6)$$

where $\rho(\nu, m^2)$ is an effective quantity, meant to repre-

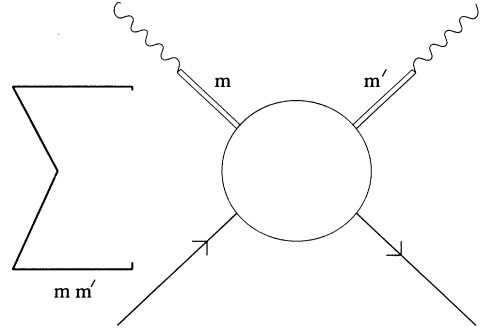


FIG. 1. The hadron dominance model Eq. (5).

sent a more complicated structure on average. Single hadronlike behavior of the intermediate states can be incorporated by assuming a Regge-type energy dependence,

$$\begin{aligned} \rho(\nu, m^2) &= \rho^P(\nu, m^2) + \rho^R(\nu, m^2) \\ &= f_P(m^2) \nu^{\alpha_P - 1} + f_R(m^2) \nu^{\alpha_R - 1}, \end{aligned}$$

where $f_P(m^2)$, $f_R(m^2)$ are smoothly varying functions of mass chosen to lead to approximate scaling at large Q^2 . In particular, if we assume

$$\rho^P(\nu, m^2) = a \nu^{\alpha_P - 1} (m^2)^{1 - \alpha_P} \quad (7)$$

for the dominant diffractive term, we have

$$F_2^P = A x \nu^{\alpha_P} \int_{m_0^2}^{\infty} dm^2 \frac{(m^2)^{1 - \alpha_P}}{(m^2 + Q^2)^2}, \quad (8)$$

where the parameters m_0 and

$$A = \frac{M a}{2 \pi^2 \alpha}$$

can be adjusted to fit the data in the “pre-HERA” region. These data have been conveniently parametrized by Donnachie and Landshoff [2] in the form

$$\begin{aligned} F_2(x, Q^2) &= F_2^P + F_2^R \\ &= A_P x^{1 - \alpha_P} \left(\frac{Q^2}{Q^2 + a_P} \right)^{\alpha_P} \\ &\quad + A_R x^{1 - \alpha_R} \left(\frac{Q^2}{Q^2 + a_R} \right)^{\alpha_R}, \end{aligned} \quad (9)$$

where

$$A_P = 0.324, \quad a_P = 0.562, \quad \alpha_P = 1.08,$$

$$A_R = 0.098, \quad a_R = 0.0111, \quad \alpha_R = 0.55. \quad (10)$$

This form was proposed on purely empirical grounds, but is very similar to parametric forms which have long been used to summarize the predictions of hadron dominance models [14]. Here we replace their F_2^P by the hadron dominance form (8), leaving the Regge component F_2^R , which is very much smaller than the diffractive term in the regions of interest, unchanged. In this way we arrive at the parametrization

³For reviews, see, for example, [14, 8], and references therein.

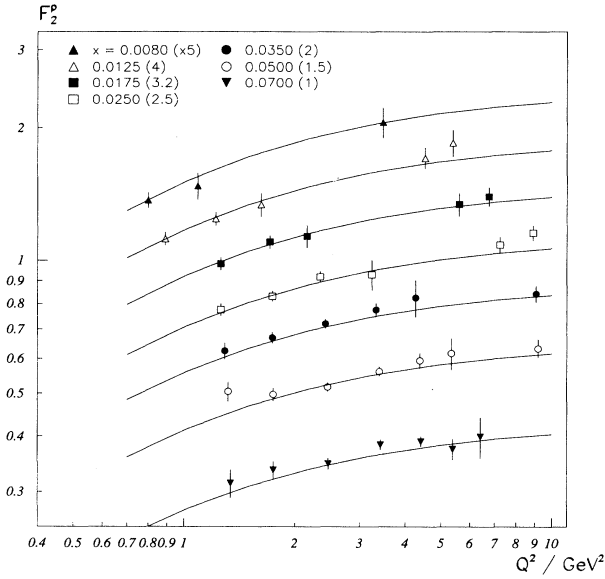


FIG. 2. Comparison of the structure function data [15] at intermediate x with the form (8) and (12) for the diffractive part, together with the Regge contribution from (9).

$$F_2 = A x \nu^{\alpha_P} \int_{m_0^2}^{\infty} dm^2 \frac{(m^2)^{1-\alpha_P}}{(m^2 + Q^2)^2} + A_R x^{1-\alpha_R} \left(\frac{Q^2}{Q^2 + a_R} \right)^{\alpha_R}. \quad (11)$$

This is a good approximation to the Donnachie-Landshoff form (9) and (10) for the choice

$$\alpha_P = 1.08, \quad m_0^2 = 0.518, \quad \text{GeV}^2, \quad A = 0.633, \quad \text{GeV}^{1.08} \quad (12)$$

of the parameters associated with the diffractive term, and by implication it gives a good account of the structure function data for $x \gtrsim 0.01$, as illustrated in Fig. 2. However, it completely fails to reproduce the HERA data

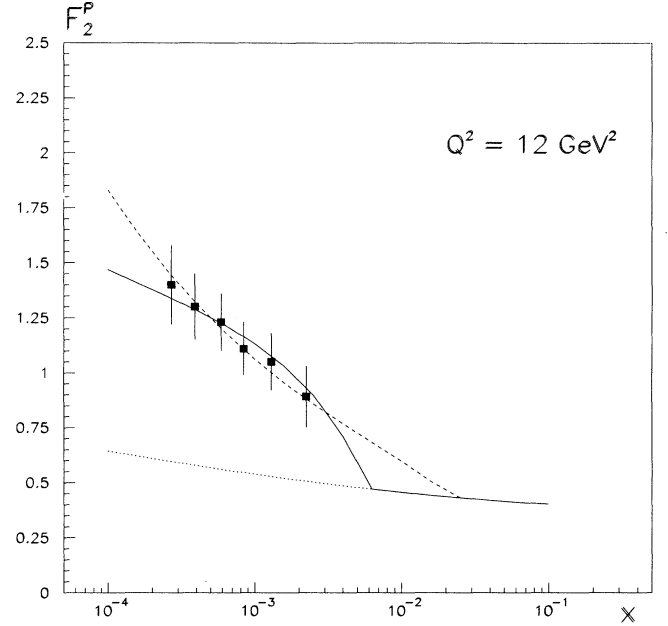


FIG. 3. Fits to the H1 data [5] at $Q^2 = 12 \text{ GeV}^2$ corresponding to fits A (solid line) and B (dashed line). The Donnachie-Landshoff parametrization (9) and (10) is shown for comparison (dotted line).

at very small x , as seen in Fig. 3, implying a transition region at $x \sim 0.01$ or somewhat lower.

The above approach embodies single hadronlike behavior $\alpha_P \approx 1.08$ for all intermediate states, and hence for the photoabsorption cross section and the structure functions. We now modify it by adjusting the contributions from $m > m_J$ and $l > l_c$, which is meant to roughly characterize the region in which single hadronlike behavior has given way to multihadronlike behavior for the intermediate states. The behavior of these states is of course very uncertain and we simply parametrize it by a form similar to (7), but with a , α_P replaced by new parameters a' , α' to be determined later. In this way we arrive at a representation of the form

$$(F_2^P)_{\text{diff}} = [\theta(m_J^2 - m^2) + \theta(m^2 - m_J^2)\theta(l_c - l)] A x \nu^{\alpha_P} \int_{m_0^2}^{\infty} dm^2 \frac{(m^2)^{1-\alpha_P}}{(m^2 + Q^2)^2} + \theta(m^2 - m_J^2)\theta(l - l_c) A' x \nu^{\alpha'} \int_{m_0^2}^{\infty} dm^2 \frac{(m^2)^{1-\alpha'}}{(m^2 + Q^2)^2}, \quad (13)$$

which is identical to our previous form (8) in the “pre-HERA” regions $\nu < \nu_c$ ($Q^2 = 0$) and $x > x_c(Q^2)$.

III. COMPARISON WITH EXPERIMENTAL DATA

Two types of fit have been explored. In the first (fit A), we impose $\alpha' = \alpha_P = 1.08$ for the high mass, long-

lived states, so that the whole of the rise at small x is due to the threshold at $l = l_c$. In the second (fit B) we assign them a steeper energy dependence $\alpha' = 1.27 > \alpha_P$ characteristic of empirical fits of the type (1) at small x , so that only part of the rise is due to the threshold effect. In both cases, the remaining parameters m_J^2 , l_c , and A were adjusted to give a reasonable fit to the HERA structure function data in the range $x < 0.01$

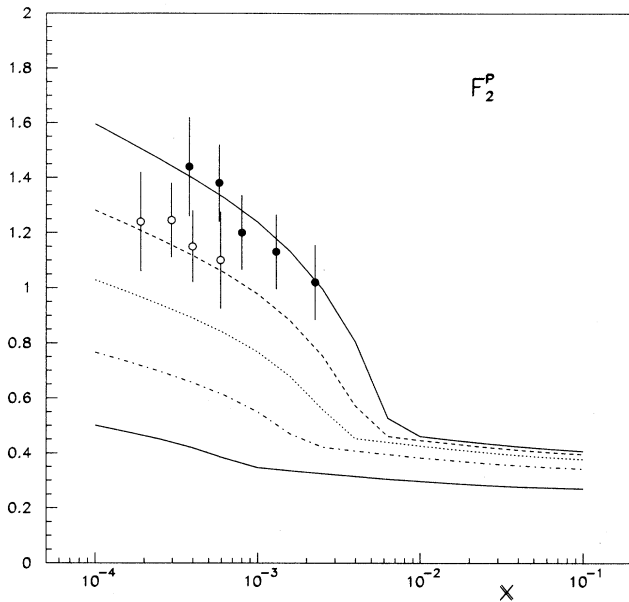


FIG. 4. Predicted structure function at small x corresponding to fit A. The data [5] correspond to $Q^2 = 15 \text{ GeV}^2$ (solid circles) and $Q^2 = 8.5 \text{ GeV}^2$ (open circles) and the curves (from the top down) to $Q^2 = 15, 8.5, 5, 2.5,$ and 1 GeV^2 , respectively.

for⁴ $8 \lesssim Q^2 \lesssim 15 \text{ GeV}^2$: essentially, m_J^2 and l_c determine the Q^2 and the x dependence of the low x enhancement, including the threshold $x_c(Q^2)$ by Eq. (4); while A determines its magnitude. The resulting values then used to predict the real photoabsorption cross section and the structure function in the unexplored region $x < 0.01$, $Q^2 \lesssim 8 \text{ GeV}^2$.

We first consider the recent H1 data [5] at small x , which are consistent with but more precise than the earlier data [3, 4]. Good fits of both types are found corresponding to the parameter values fit A: $\alpha' = 1.08$,

$$m_J^2 = 16 \text{ GeV}^2, \quad l_c = 15 \text{ fm}, \quad A' = 2.7 \text{ GeV}^{1.08}, \quad (14)$$

fit B: $\alpha' = 1.27$,

$$m_J^2 = 8 \text{ GeV}^2, \quad l_c = 6 \text{ fm}, \quad A' = 0.62 \text{ GeV}^{1.08}, \quad (15)$$

respectively. These are compared in Fig. 3 for $Q^2 = 12 \text{ GeV}^2$, while the predicted Q^2 dependence is shown in Figs. 4 and 5. As can be seen, an enhancement of the desired form is obtained, which is confined to small⁵

⁴We restrict ourselves to $Q^2 \lesssim 15 \text{ GeV}^2$ since we are interested in the transition region from real photons to deep inelastic behavior. The Donnachie-Landshoff parametrization (9) and (10) is a good fit to the intermediate x data in this same Q^2 region, but will of course break down eventually since it gives exact scaling as $Q^2 \rightarrow \infty$.

⁵Because we have for simplicity used θ functions to separate the different regions in (13), there is a discontinuity in the derivative of $F_2(x)$ at $x = x_c$. This could easily be smoothed slightly by using gentler thresholds, but given the accuracy of the data, this is not necessary.

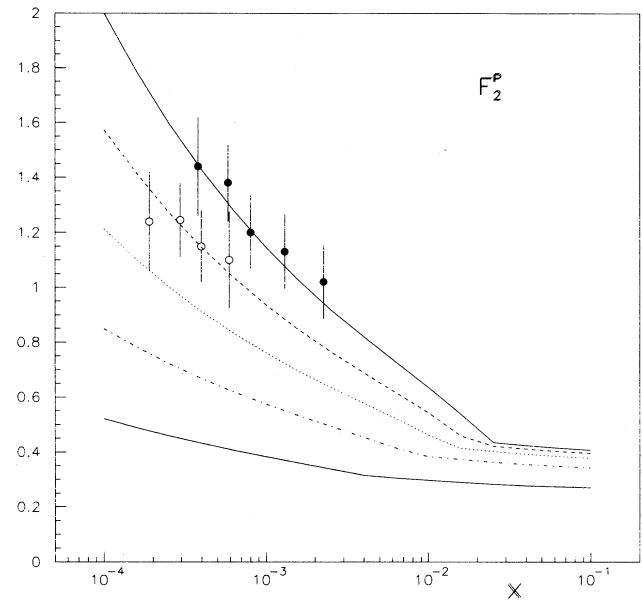


FIG. 5. Predicted structure function at small x corresponding to fit B. The data [5] correspond to $Q^2 = 15 \text{ GeV}^2$ (solid circles) and $Q^2 = 8.5 \text{ GeV}^2$ (open circles) and the curves (from the top down) to $Q^2 = 15, 8.5, 5, 2.5,$ and 1 GeV^2 , respectively.

$x < x_c(m_J, l_c, Q^2)$. Because of this, the fit to the intermediate- x data of Fig. 2 is either completely unchanged (fit A) or very slightly modified at the highest Q^2 values for the lowest x values without spoiling the agreement with experiment (fit B) [16].

The corresponding predictions for the real photoab-

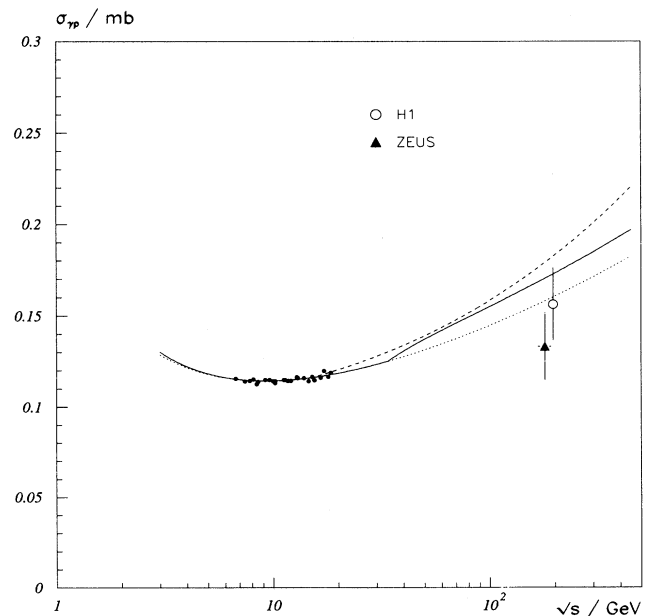


FIG. 6. Fits to the real photoabsorption data corresponding to fits A (solid line) and B (dashed line). The Donnachie-Landshoff parametrization (9) and (10) is shown for comparison (dotted line).

sorption cross sections [17–19] are shown in Fig. 6. As can be seen, the enhancement from the high mass, long-lived states is confined to high energies and is relatively small. Nonetheless the predictions are a little high compared to the ZEUS data, especially for fit *B*. The source of this problem is clear: the cross section that follows from the Donnachie-Landshoff form (9) and (10) already completely saturates the experimental high energy cross section. Since our basic vector mesonlike contributions have been constructed to reproduce this parametrization, and we have then enhanced them at large masses and large coherence lengths, some disagreement is inevitable. The key point is that if it is not too large, one could hope to correct it by slightly modifying the parameters of the conventional hadronlike contributions, so that they still fit the “pre-HERA” data but do not already saturate the real photoabsorption cross section at very high energies. One simple but not unique way to do this is to lower α_P slightly, and then repeat the analysis.

Since we follow the same procedure as before, we shall summarize it rather briefly. The pre-HERA data are still well fitted if the parameters in the Donnachie-Landshoff form (9) are replaced by

$$\begin{aligned} A_P &= 0.350, & a_P &= 0.530, & \alpha_P &= 1.06, \\ A_R &= 0.073, & a_R &= 0.010, & \alpha_R &= 0.55. \end{aligned} \quad (16)$$

Again we retain the Regge component F_2^R but replace the dominant diffractive component F_2^D by a hadron dominance representation (8) with parameters

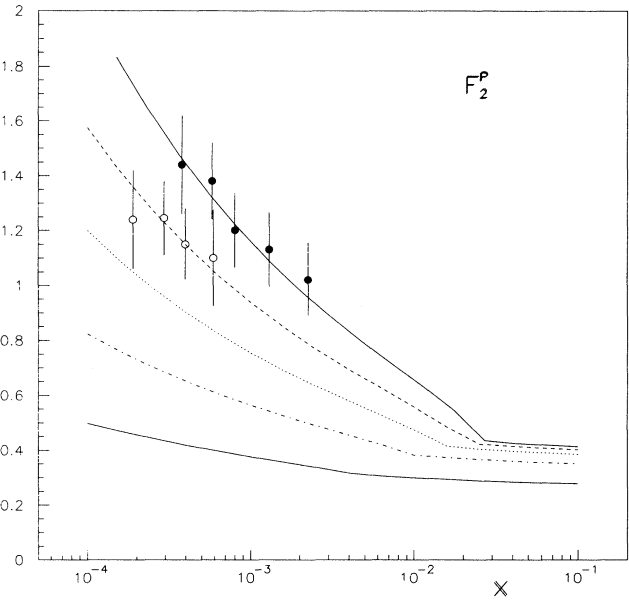


FIG. 8. Predicted structure function at small x corresponding to fit *B'*. The data [5] correspond to $Q^2 = 15 \text{ GeV}^2$ (solid circles) and $Q^2 = 8.5 \text{ GeV}^2$ (open circles) and the curves (from the top down) to $Q^2 = 15, 8.5, 5, 2.5,$ and 1 GeV^2 , respectively.

$$\alpha_P = 1.06, \quad m_0^2 = 0.499, \quad \text{GeV}^2, \quad A = 0.679 \text{ GeV}^{1.06}, \quad (17)$$

We then modify the behavior of the heavy, long-lived states in accordance with our final representation (13) and obtain two different fits as before corresponding to

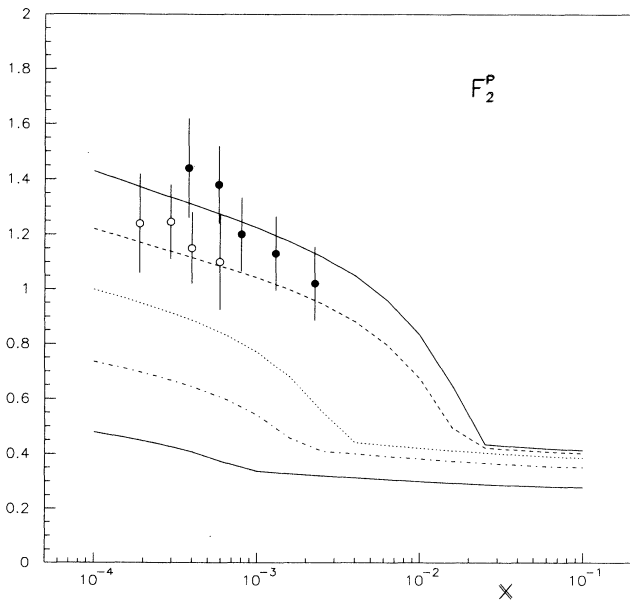


FIG. 7. Predicted structure function at small x corresponding to fit *A'*. The data [5] correspond to $Q^2 = 15 \text{ GeV}^2$ (solid circles) and $Q^2 = 8.5 \text{ GeV}^2$ (open circles) and the curves (from the top down) to $Q^2 = 15, 8.5, 5, 2.5,$ and 1 GeV^2 , respectively.

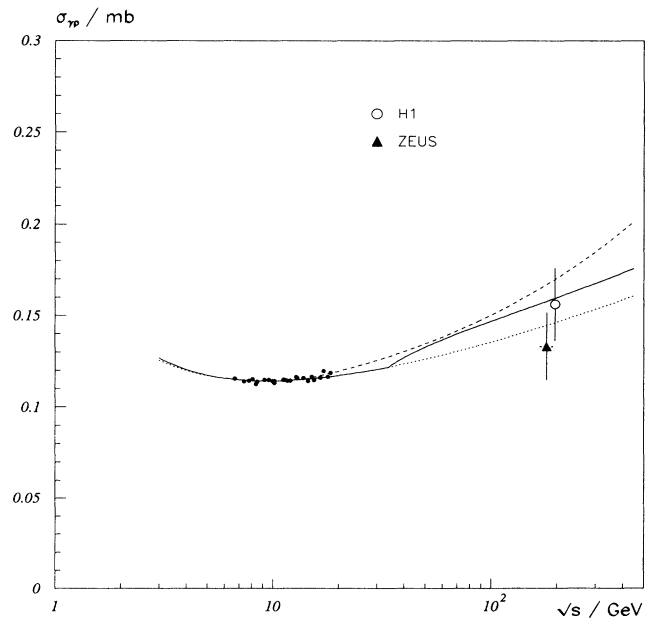


FIG. 9. Fits to the real photoabsorption data corresponding to fits *A'* (solid line) and *B'* (dashed line). The modified Donnachie-Landshoff parametrization (9) and (16) is shown for comparison (dotted line).

the parameter values fit A' : $\alpha' = 1.06$

$$m_J^2 = 16 \text{ GeV}^2, \quad l_c = 15 \text{ fm}, \quad A' = 3.2 \text{ GeV}^{1.06}, \quad (18)$$

fit B' : $\alpha' = 1.27$,

$$m_J^2 = 8 \text{ GeV}^2, \quad l_c = 5 \text{ fm}, \quad A' = 0.64 \text{ GeV}^{1.27}, \quad (19)$$

respectively. The corresponding fits to the structure function data at low x are shown in Figs. 7 and 8, and are very similar to our previous fits A and B . However the predictions for real photoabsorption are now in good agreement with the data, as shown in Fig. 9.

IV. SUMMARY

Real photoabsorption and proton structure function data at small x exhibit very different energy dependence at fixed Q^2 . Here we have shown that both can be well described by a simple hadron dominance model in which the striking enhancement observed at HERA at very low x and high Q^2 is attributed to contributions from heavy

long-lived fluctuations of the incoming photon. Two contrasting assumptions on the energy dependence of the scattering of these states by the proton have been made, leading to fits which differ at very small $x \lesssim 10^{-4}$ as can be seen in Fig. 3. However they are very similar for the range $2 \times 10^{-4} < x \lesssim 2 \times 10^{-3}$ and $Q^2 \gtrsim 8 \text{ GeV}^2$, in which the well-known small x enhancement has been observed at HERA. The most important predictions concern the behavior of this enhancement in the intermediate Q^2 range $0 < Q^2 \lesssim 6 \text{ GeV}^2$, which has not yet been explored experimentally. The fits give similar results for this Q^2 dependence in the relevant x region $2 \times 10^{-4} < x \lesssim 2 \times 10^{-3}$, as can be seen by comparing Figs. 4 and 5; and as Q^2 becomes smaller, the effect is predicted to decrease rapidly and shift towards $x = 0$.

ACKNOWLEDGMENT

One of us (G.S.) would like to thank Professor D. Schildknecht for a series of extremely helpful discussions on this topic.

-
- [1] A. Donnachie and P.V. Landshoff, Phys. Lett. B **296**, 227 (1992).
 - [2] A. Donnachie and P.V. Landshoff, Z. Phys. C **61**, 139 (1994).
 - [3] H1 Collaboration, I. Abt *et al.*, Nucl. Phys. **B407**, 515 (1993).
 - [4] ZEUS Collaboration: M. Derrick *et al.*, Phys. Lett. B **316**, 412 (1993).
 - [5] H1 Collaboration: in *Proceedings of the 27th International Conference on High Energy Physics*, Glasgow, Scotland, 1994, edited by P. J. Bussey and I. G. Knowles (IOP, London, 1995).
 - [6] A.D. Martin, R.G. Roberts, and W.J. Stirling, Phys. Rev. D **50**, 6734 (1994).
 - [7] Y.Y. Bulitsky and L.N. Lipatov, Sov. J. Nucl. Phys. **28**, 822 (1978); E.A. Kuraev, L.N. Lipatov, and V.S. Fadin, Sov. Phys. JETP **45**, 199 (1977).
 - [8] G. Shaw, Phys. Lett. B **318**, 221 (1993).
 - [9] ZEUS collaboration, in *Proceedings of the 27th International Conference on High Energy Physics*, [5].
 - [10] P. Moseley and G. Shaw, J. Phys. G **21**, 1043 (1995).
 - [11] M. Arneodo, Phys. Rep. **240**, 301 (1994).
 - [12] G. Shaw, Phys. Rev. D **47**, R3676 (1993).
 - [13] V. Del Duca, S.J. Brodsky, and P. Hoyer, Phys. Rev. D **46**, 931 (1992).
 - [14] For a review and references to the early literature on this subject, see A. Donnachie and G. Shaw, in *Electromagnetic Interactions of Hadrons*, edited by A. Donnachie and G. Shaw (Plenum, New York, 1978), Vol. 2.
 - [15] New Muon Collaboration, P. Amaudruz *et al.*, Phys. Lett. B **295**, 159 (1992).
 - [16] These and other details of the various fits are given explicitly in P. Moseley, M.Sc. dissertation, University of Manchester, 1994.
 - [17] Particle Data Group, Phys. Rev. D **45**, 51 (1992).
 - [18] H1 Collaboration, in *Proceedings of the International Europhysics Conference on High Energy Physics*, Marseilles, France, 1993, edited by J. Carr and M. Perottet (Editions Frontieres, Gif-sur-Yvette, 1993), p. 793.
 - [19] ZEUS Collaboration, *Proceedings of the International Europhysics Conference on High Energy Physics*, [18], p. 811.